Spin-dependent electron transmission through bacteriorhodopsin embedded in purple membrane

Debabrata Mishra[a,1], Tal Z. Markus[a,1], Ron Naaman[a,2], Matthias Kettner[b], Benjamin Göhler[b], Helmut Zacharias[b,2], Noga Friedman[c], Mordechai Sheves[c], and Claudio Fontanesi[d,2]

Departments of [a]Chemical Physics and [c]Organic Chemistry, Weizmann Institute, Rehovot 76100, Israel; [b]Physikalisches Institut, Westfälische Wilhelms-Universität Münster, 48149 Münster, Germany; and [d]Department of Chemistry, University of Modena, 41100 Modena, Italy

Edited by Harry B. Gray, California Institute of Technology, Pasadena, CA, and approved August 2, 2013 (received for review June 17, 2013)

Spin-dependent photoelectron transmission and spin-dependent electrochemical studies were conducted on purple membrane containing bacteriorhodopsin (bR) deposited on gold, aluminum/aluminum-oxide, and nickel substrates. The result indicates spin selectivity in electron transmission through the membrane. Although the chiral bR occupies only about 10% of the volume of the membrane, the spin polarization found is on the order of 15%. The electrochemical studies indicate a strong dependence of the conduction on the protein's structure. Denaturation of the protein causes a sharp drop in the conduction through the membrane.

electron transfer | electrochemistry | magnetic effect | chirality

The role of the electron spin in chemistry and biology has been receiving much attention because of a plausible relation to electromagnetic field effects on living organisms (1), and due to the seemingly importance of the earth's magnetic field on birds and fish navigation (2). Part of the difficulty in studying the subject arises from the lack of a physical model that can rationalize these phenomena. Recently, the chiral-induced spin selectivity (CISS) effect was observed in electron transmission and conduction through organic molecules (3). The spin selectivity was observed for photoelectron transmission through monolayers of double-stranded DNA adsorbed on gold (4). Another study discovered a spin dependence in the conduction through single molecules of double-stranded DNA. In this configuration, one end of the molecule was adsorbed on a Ni substrate, whereas the other was attached to a gold nanoparticle (5).

The CISS effect may provide a novel approach for better understanding the role of electron spin in biological systems. The studies mentioned above led to several questions, including the actual role played by the gold substrate in the overall spin-filtering process. Gold exhibits a very large spin orbit coupling; hence, one may wonder whether gold itself affects the CISS phenomenon. In addition, the interface between gold and the thiol group, through which the molecules are attached to the gold, may play a role. Because many of the past studies were performed with DNA, an important question arises whether CISS is a general effect or possibly a special property of DNA. CISS was only observed for double-stranded DNA, whereas for single-stranded molecules, no spin selectivity was found. On the one hand, this was attributed to the lack of ordered monolayers (4, 6); on the other hand, a theoretical model, proposed to rationalize the CISS effect, predicted that a double-helix structure (7) was needed for CISS to occur, whereas other approaches do not emphasize this need (8). Finally, because many of the past studies were performed in vacuum or in ambient air, it is of importance to probe to what extent the effect persists in solutions, which are more relevant to biology. The present study aims at answering the above questions in an attempt to establish CISS as a general phenomenon.

For the present study, we chose bacteriorhodopsin (bR) as a chiral system, which is a transmembrane protein composed of seven parallel, upright-oriented α-helices. The protein is embedded in its native membrane environment so that it will resemble most closely its natural structure (Fig. 1*A*). Electron conduction through these purple membranes was measured recently (9) in ambient and as a function of temperature (10). Electrochemical and conduction studies were also performed when the purple membranes were deposited on gold (11).

In the present study, the purple membrane, that includes about 10% in volume of the protein, was physisorbed on either gold, aluminum (with its native oxide), or Ni substrates in an inert atmosphere. Morphology and coverage of the bR were characterized by field emission SEM (FE-SEM). To confirm that the protein lies perpendicular to the membrane surface, we took the image of an isolated bR patch by atomic force microscopy and found that the height h of an individual patch is $h \sim 49$Å, which approaches the standard height of bR standing upright inside the membrane. Circular dichroism spectra were taken before the experiment to confirm that bR retains the helical structure in the deposited membrane and that there is no change in conformation as a result of deposition on a metal substrate (see *SI Appendix*).

Two different methods were applied for monitoring the CISS effect in bR. The first is to analyze the spin polarization of photoelectrons ejected from a substrate that is coated with bR. We previously applied this technique in studying spin-dependent electron transmission through monolayers of double-stranded DNA self-assembled on gold (4). UV radiation with photon energy below the ionization potential of the adsorbed molecules, but above the work function of the substrate, excites photoelectrons

Significance

The role of the electron spin in chemistry and biology has been receiving much attention because of a plausible relation to electromagnetic field effects on living organisms. Part of the difficulty in studying the subject arises from the lack of a physical model that can rationalize these phenomena. Recently the chiral-induced spin selectivity effect was observed in electron transmission through organic molecules. The question is to what extent the effect takes place in proteins. In the present study, we probed bacteriorhodopsin embedded in its native membrane environment. We observed clear evidence for spin-dependent electron transmission through this system. The results point to the possibility that the effect may play a role in electron transfer in biological systems.

Author contributions: R.N. and H.Z. designed research; D.M., T.Z.M., M.K., B.G., and C.F. performed research; N.F. and M.S. contributed new reagents/analytic tools; R.N., H.Z., and M.S. analyzed data; and D.M., R.N., B.G., H.Z., M.S., and C.F. wrote the paper.

The authors declare no conflict of interest.

This article is a PNAS Direct Submission.

Freely available online through the PNAS open access option.

[1]D.M. and T.Z.M. contributed equally to this work.

[2]To whom correspondence may be addressed. E-mail: ron.naaman@weizmann.ac.il, h.zacharias@uni-muenster.de, or claudio.fontanesi@unimore.it.

This article contains supporting information online at www.pnas.org/lookup/suppl/doi:10.1073/pnas.1311493110/-/DCSupplemental.

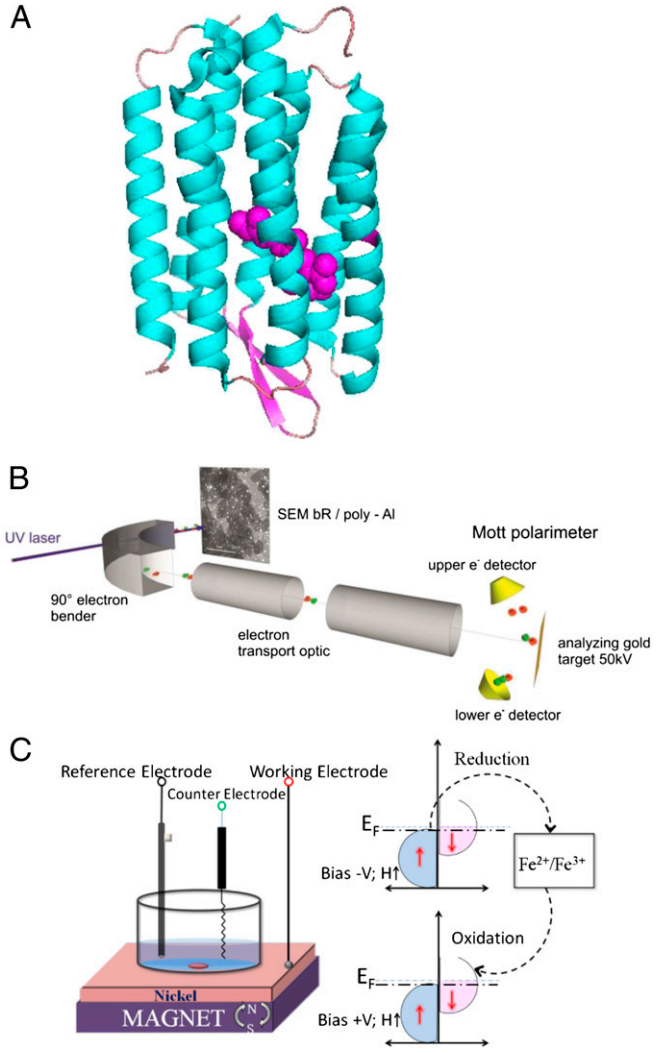

Fig. 1. (*A*) Structure of the bR. (*B*) Spin-dependent photoelectrons' experimental setup. UV laser radiation (blue) excites photoelectrons from a bR-coated poly-Al substrate. Here a scanning electron microscope image of a partial monolayer is shown. The excited electrons are extracted antiparallel to the light incidence, bent by 90°, and guided into the Mott polarimeter to determine their longitudinal spin polarization. (*C*) (*Left*) Spin-dependent electrochemistry setup. The working electrode is made from nickel; underneath, a magnet is placed whose direction can be flipped. (*Right*) Scheme of the energy levels in the magnetized nickel. In the reduction process, electrons with the majority spin are ejected from the electrode, whereas in the oxidation stage, electrons with the minority spin are inserted.

in the substrate. These electrons are transmitted through the layer of adsorbed molecules and analyzed in the vacuum with regard to their kinetic energy using a time-of-flight spectrometer or by a Mott polarimeter for determining their spin polarization. Such experiments have been performed for patches of purple membrane deposited either on poly-Au or on Al/AlO_x substrates.

The second method applied was spin-dependent cyclic voltammetry (CV). Here, the patches of purple membranes were deposited on a Ni substrate, and the current through them was monitored as a function of the direction of the magnetization of the supporting Ni that was altered by applying an external magnetic field using a permanent magnet.

The results presented here indicate very efficient spin filtering by bacteriorhodopsin, both for photoelectron transmission and for conduction. It was also shown that the substrate does not affect the CISS and that it also exists when the sample is deposited on a material with very low spin-orbit coupling. Furthermore, the results prove that the chiral molecules do not need to be chemically bound to the surface for the effect to be observed. Finally, the effect exists even if the membrane that contains the chiral protein is imbedded in solution.

Results and Discussion

Spin-Dependent Photoelectron Transmission. The experimental system was described in detail in ref. 4. However, the experimental setup was improved with regard to the vacuum conditions by replacing a plastic insulator of the Mott polarimeter by a metal sealed ceramic. Fig. 1*B* schematically shows the important components of the system.

The electron spin polarization is defined by $P = \frac{I_+ - I_-}{I_+ + I_-}$, where I_+ and I_- are the signals for electrons with their spin aligned parallel or antiparallel to their velocity vector, respectively. The results for bR imbedded in the purple membrane deposited on gold are shown in Fig. 2 for a submonolayer of patches of the membrane (*Left*) and for gold covered completely with patches of the membrane (*Right*). In the case of submonolayer coverage, a spin polarization of $P = 5 \pm 3\%$ was found, whereas for the completely covered gold, the polarization amounts to $P = 14 \pm 5\%$. More than 10 different samples were measured, for which the method of preparation varied somewhat (see *SI Appendix*). Careful inspection of the data in the left panel of Fig. 2 indicates that the polarization of the laser light, applied for ejecting the photoelectrons from gold, has a small effect on the spin-polarization measured. This effect is due to the electrons ejected from gold being spin polarized according to the laser polarization. It is important to realize that circularly polarized light excites spin-polarized electrons from clean gold and that the sign depends on the helicity of the light, whereas linearly polarized light excites unpolarized photoelectron (0% spin polarization) ensembles only (e.g., supplemental material of ref. 4). When, however, the gold substrate is covered with bR, the sign of the electron spin polarization is always positive, independent of the polarization of the exciting radiation (Fig. 2). However, the light polarization influences the magnitude of the spin polarization. Clockwise (CW) circularly polarized light excites electrons, which with $P = 17 \pm 5\%$, have the (in absolute values) highest spin polarization after transmission through the purple membrane, because these electrons already have a positive spin polarization when excited from the bare poly-Au substrate. Electrons excited by linearly polarized light, which are initially unpolarized when excited from a clean substrate, exhibit less spin polarization: $P = 14 \pm 5\%$. The spin polarization is even smaller when counterclockwise (CCW) circularly polarized light is used for the excitation: $P = 8 \pm 5\%$. This polarization results from photoelectrons excited from bare polycrystalline gold by CCW circularly polarized light, which is negatively spin-polarized. After transmission of the electrons through bR, a predominant alignment of electron spin orientation parallel to their direction of propagation (positive spin polarization) is observed. Therefore, one can conclude that the protein within the membrane does polarize transmitted electrons and that its effect prevails. The initial polarization of the electrons before entering the membrane has only a minor effect on the final spin polarization.

Fig. 3 displays results obtained with an aluminum substrate. Here the spin polarization observed for the completely covered surface is $P = 15 \pm 4\%$. As expected, no effect of the laser polarization can be detected, because the spin polarization of photoelectrons ejected from the aluminum does not vary with the laser light polarization. Owing to weak spin-orbit coupling in Al (0.12 eV compared with 4.54 eV for gold), circularly polarized light does not excite spin-polarized electrons.

In the case of bR, the electron spin polarization found is positive, whereas in the studies of photoelectron transmission

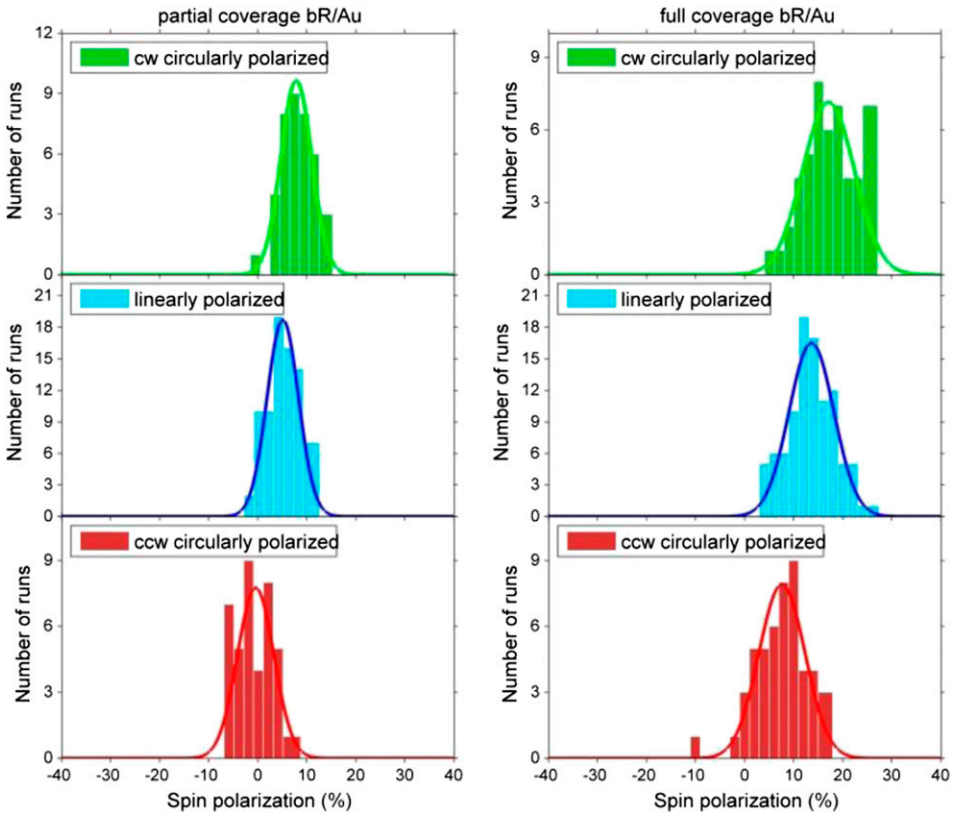

Fig. 2. Spin polarization measured for photoelectrons, which are ejected by clockwise (cw, green), counterclockwise (ccw, red), circularly, and linearly (blue) polarized laser radiation, after having traversed a purple membrane containing bR 10% in volume adsorbed on gold. When the photoelectrons are ejected from gold substrates, a spin polarization of, on average, about $P = 5\%$ and $P = 14\%$ is measured for partial (*Left*) and completely covered surfaces (*Right*), respectively.

through double-stranded DNA, the electron spin polarization has a negative sign. It means that the preferred spin in the electron transmission is opposite in both cases. Currently, there is no theory that explains this observation. However, the observed difference may be explained by the environment as was also observed in circular dichroism (CD) spectroscopy (12). Namely, whereas with DNA the electrons traverse a layer made entirely from DNA, with the bR, the protein is imbedded within phospholipids and hence the transmitted electron interacts not only with the electrons on the helices but also with the electronic structure of the "cage" formed by the phospholipids composing the membrane.

Spin-Dependent Electrochemistry. The influence of the spin on electron conduction through the purple membrane has been probed by recording CV curves as a function of the magnetization of a Ni substrate supporting the purple membrane. The redox couple selected for the current study was 1 mM $K_4[Fe(CN)_6]/K_3[Fe(CN)_6]$ (Fe^{2+}/Fe^{3+}) due to its robust chemical properties and to the well-documented and thorough knowledge of its thermodynamic, kinetic, and electrochemical parameters. The relevant chemical reaction is a reversible electrochemical equilibrium. The relevant standard potential is $E^0 = +0.120$ V vs. saturated calomel electrode (SCE):

$$Fe(CN)^{3+}_{6\ (solution)} + e^- \rightleftharpoons Fe(CN)^{2+}_{6\ (solution)}.$$

The study was performed in an aqueous solution at pH = 7 [Tris (hydroxymethyl)aminomethane (Tris) buffer] containing 50 mM NaCl and 50 mM $MgCl_2$.

Fig. 4*A* shows CVs recorded on the bare Ni surface featuring roughly 2 nm of thermal oxide, NiO, on the surface. The oxidation and reduction current peaks are separated by 90 mV, at a scan rate of 50 mV/s. The CVs are recorded in the scanning potential range from −0.05 to +0.35 V, which is within the Ni double layer potential window, the latter ranging between the hydrogen evolution (−0.60 V) and the nickel oxidation potential (+0.45 V) (13–15). The forward potential scan from −0.05 to +0.35 V involves Fe^{2+} oxidation, whereas the backward scan involves Fe^{3+} reduction. Note that CVs of the Fe^{2+}/Fe^{3+} couple are often used to probe the extent of oxidation of the surface of the electrode (16, 17). Both the current and the potential peak-to-peak difference (the theoretical peak-to-peak difference being 58 mV) are strongly dependent on the extent of oxidation of the surface, i.e., the electrical conduction characteristics of the solution/interface/electrode system.

Fig. 4*B* shows CV curves recorded when the Ni substrate is covered with the purple membrane containing the bR for different external magnetic field directions. The CV curves are characterized by "quasi-reversible" behavior, definitively different from the CVs recorded on the bare Ni surface (Fig. 4*A*). In fact, the neat current peaks (featuring a 90-mV potential separation) in Fig. 4*A* are replaced by broad oxidation and reduction shoulders including a larger separation in the potential values. Shoulders are roughly found at +0.250 V in the forward oxidation curve and at +0.075 V in the backward reduction curve. This behavior is commonly observed when charge transfer through adsorbed molecular films takes place, as is found in the case of CV performed with surfaces coated with self-assembled monolayers of α-helical peptides (18). Thus, the modification in the CV curves from a reversible (Fig. 4*A*) to a quasi-reversible

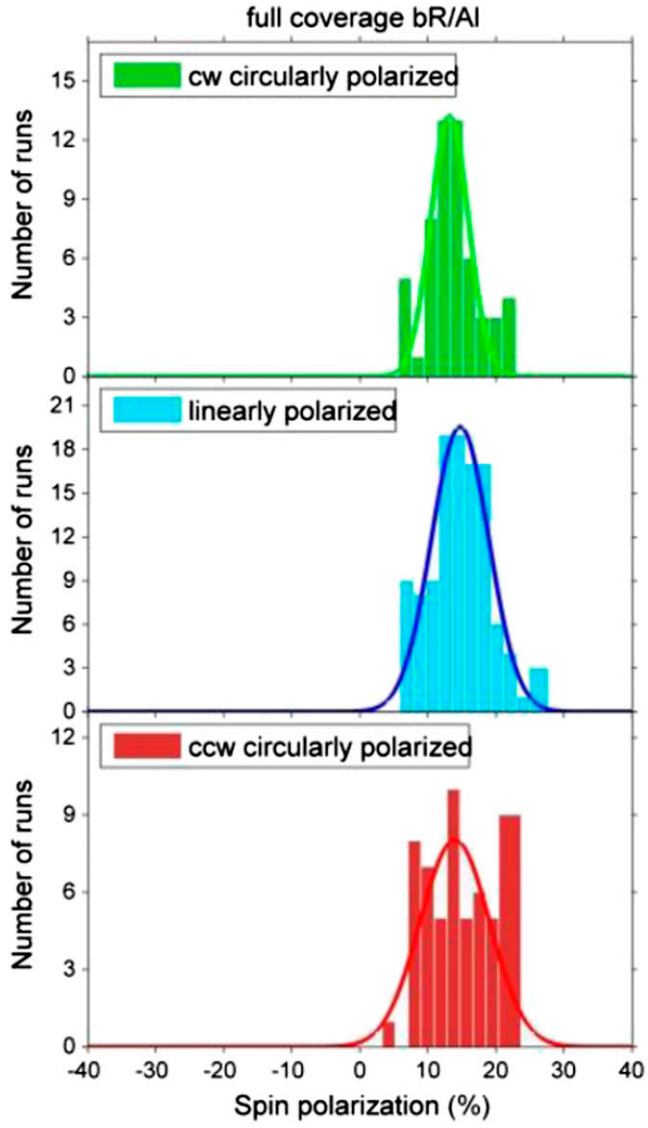

Fig. 3. Spin polarization measured for photoelectrons that are ejected from aluminum by clockwise (cw, green), counterclockwise (ccw, red), circularly, and linearly (blue) polarized laser radiation, after having traversed a purple membrane containing bR 10% in volume. When the electrons were ejected from aluminum substrates, a spin polarization of about $P = 15\%$ was measured.

(Fig. 4*B*) state is due to the low electrical conduction of the purple membrane.

The current in Fig. 4*B* is almost one order of magnitude lower than that recorded for the bare Ni surface (Fig. 4*A*). The CVs recorded as a function of the magnetic field direction exhibit a systematic difference in the current, which suggests that the electron transfer through bR (electronic conduction) depends on the spin orientation. Moreover, the difference between the CV currents, recorded in the magnet UP (Fig. 4*B*, red curve) and magnet DOWN (Fig. 4*B*, blue curve), is a function of the applied potential; thus, a quantitative comparison of the current values should be performed at a fixed potential. Remarkably, an average difference of $18 \pm 3\%$ was observed between the currents relevant to the magnet UP and magnet DOWN configurations, determined at the initial (−0.10 V) and final (+0.35 V) CV curve. The difference in the current, ΔI, for the two directions of the magnet is $\Delta I = 1.3$ μA at −0.05 V, corresponding to a difference of about 21%, and $\Delta I = 1.5$ μA at +0.35 V, namely, a difference of 18.8%. The *Inset* in Fig. 4*B* shows CV curves recorded (*i*) before and (*ii*) after a −1.0 to +1.0 V CV scan. The curves were measured on a different sample than that used for obtaining the curves in Fig. 4*B*, and therefore the current ranges from −20 to +20 mA, higher than that measured for the sample probed in Fig. 4*B*. The dramatic drop in the current, following the application of the wide −1.0 to +1.0 V potential window, is due to the denaturation of the protein in the membrane (19, 20). This denaturation was probed by monitoring the absorption and CD spectra of the bR-containing purple membrane before and after applying the −1.0 to 1.0 CV scan (see *SI Appendix*). Following the application of the high voltage, the absorption spectrum changes to that of free retinal, a change occurring on denaturation of the protein, and there is no measureable CD signal. The CV recorded after the denaturation of the bacteriorhodopsin (curve *ii* in Fig. 4*B*, *Inset*) shows an almost constant and close to zero current, thus indicating that the lipid film framework is still physisorbed on the Ni surface and that the conduction observed in Fig. 4*B* and in *Inset* curve i occurs primarily through the bR imbedded in the membrane. If the membrane would be removed, one would expect to observe a curve similar to the in Fig. 4*A* that includes the redox peak. The fact that this is not observed is a clear indication that the electrode is still covered, but now the adsorbed layer does not conduct well electrons. Note that CV curves in the *Inset* are still recorded in the double-layer Ni potential window (vide supra); thus, surface Ni oxidation or hydrogen evolution processes are excluded.

The results indicate that conduction through the membrane is facilitated by the helical structure of the protein. Concerning the possible role played by defects present in the bR film, like pinholes, it must be emphasized that the actual geometrical rearrangement of the electrochemical cell, relevant to the measurement of the CVs, features only the flipping of the magnet, whereas the solution/bR interface spatial disposition is left unchanged. Therefore, possible strain contributions due to direct contact between the solution containing the redox probe and the nickel surface remain constant with respect to the UP and DOWN positions of the magnet.

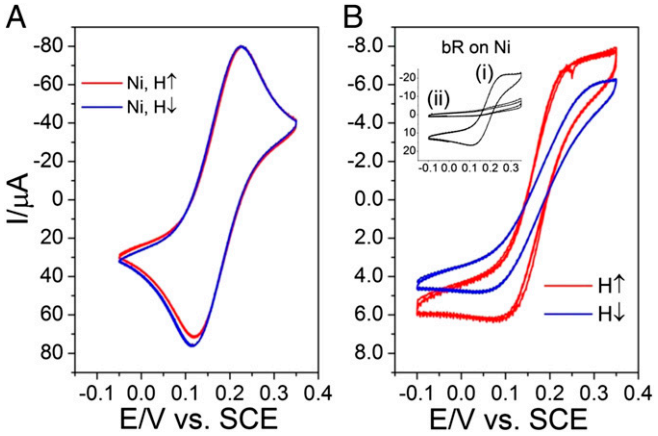

Fig. 4. CV curves of the 1 mM $K_4[Fe(CN)_6]/K_3[Fe(CN)_6]$ redox couple in a pH = 7 (Tris)-buffered, 50 mM NaCl, and 50 mM $MgCl_2$ base electrolyte, aqueous solution: Initial potential = −0.05 V; final potential = +0.35 V; scan rate = 50 mV/s. (*A*) CV for a Ni bare surface as a working electrode. (*B*) CV obtained using the bR thin film physisorbed on the Ni working electrode; arrows in the figures indicate the two possible directions (conventionally UP and DOWN) of the magnetic field ($H = 0.35T$), which is orthogonal to the surface of the working electrode. (*Inset*) CVs of a bR/Ni thin film at $H = 0$: (*i*) freshly deposited bR on Ni and (*ii*) after the electrochemical burning of the bR (see the text for the experimental details).

Thus, their contributions, if any, do not affect the difference in the current found in the UP vs. DOWN magnet direction.

There were four questions presented in the introduction. What is the role of the gold? What is the role of the bonding to the surface? Does the effect exist only in double-stranded DNA? Does the effect take place also in solution? The results presented here provide answers to all of the questions. Clearly, the CISS effect results from the chiral system itself and is independent of the substrate; we observe it also on Al, which has very small spin-orbit coupling. The membranes studies are physisorbed on the surface; hence, the substrate–molecule bond is not essential for observing the effect. The effect observed indicates that the spin selectivity is very high for electron transmission above the vacuum level (photoelectrons), for the electron conduction (in DNA) (5), and for the CV measurements performed in solution. Because the protein is in its native form and is in an environment not too different from in vivo, the results point to the possibility that the CISS effect takes place in biological systems and specifically plays a role in electron transfer through helical proteins. There the CISS effect may reduce the electron backscattering by the coupling between the spin and the electrons' linear momentum (21). Hence, the CISS effect could make electron transfer through helical proteins more efficient.

Methods

Membrane Preparation and Deposition. The purple membrane patches were prepared according to previously described methods (22, 23).

Gold, aluminum, and Ni thin films of thicknesses of about 150 nm were grown by an e-beam evaporator at a pressure of 10^{-6} Torr at room temperature in a clean room. The deposition rate and power of the beam were adjusted to form a uniform surface. As-grown thin films were carefully kept in an inert atmosphere. Seventy microliters of bR in patch suspensions (suspended in water with a concentration of 0.4 OD) was drop cast on thin film of size 10 × 10 mm. The whole system was kept for 15 min in vacuum, and then it was gently washed with water to form the monolayer on a metal substrate. For the formation of multilayers, the bR solution on the Al or Ni substrate was kept in a desiccator with continuous pumping by a roughing pump. The whole system was kept in vacuum for 48 h to form the multilayer of bR on the thin film. Surface coverage and morphology of the surface was characterized by FE-SEM.

Circular dichroism spectra of bR films were measured using a Chirascan spectrometer (Applied Photo Physics). The measurement conditions were as follows: scan, 180–260 nm; time per point, 1 s; step size, 1 nm; bandwidth, 1 nm; 18 repeats.

Photoelectron Spectroscopy. Photoelectrons are excited with a laser radiation of adjustable polarization. A diode-pumped active mode-locked Nd:YVO_4 oscillator is regeneratively amplified (diode-pumped Nd:YVO_4) at a repetition rate of 20 kHz. Applying nonlinear frequency conversion, the fifth harmonic at 212.8 nm ($h\nu = 5.84$ eV) is obtained with a pulse energy of about 5 μJ, of which only a very small fraction is used in the experiment to prevent sample damage and charging. The polarization of the laser light can be changed by rotating a quarter wave plate to obtain either CW, CCW, circularly, or linearly polarized light. A distortion in the circularity of the polarization was carefully checked and found to be less than 2% relative to the change in the ellipticity.

The spin polarization of the photoelectrons is analyzed by applying a Mott polarimeter. To prevent the spin orientation of the photoelectrons from being influenced by the earth's magnetic field, it is compensated with a three-axis Helmholtz coil setup, and the vacuum chamber is also equipped with a μ-metal shield. In the calibrated Mott polarimeter, the electrons are accelerated by 50 kV onto a gold target, and an asymmetry A is measured between two symmetric detectors that count the backscattered electrons at a 120° scattering angle. This asymmetry A is proportional to the spin polarization P, $A = P \cdot S_{eff}$, where the analyzing power (effective Sherman function) S_{eff} has been calibrated to 18%.

To determine the absolute spin polarization of samples that are not allowed to reverse the sign of the spin polarization (e.g., by changing the helicity of the exciting laser radiation), a reference method is used that has been previously described in detail in the supplemental material of ref. 4.

Electrochemistry. CV measurements were performed using a 263A PAR potentiostat and a typical three-electrode electrochemical cell arrangement, without any electrolyte solution ohmic drop correction. A 50 mM NaCl and 50 mM $MgCl_2$ solution was used as the supporting electrolyte in aqueous solution, which was Tris buffered and had a pH = 7. Ni evaporated on Si, a Pt wire, and a SCE were used as the working, counter, and reference electrodes, respectively. The Ni surface was secured to the bottom of a Teflon cell through an O-ring of 0.8 cm diameter. The body of the Teflon cell, as well as all of the remaining glassware used in the electrochemical experiments, was cleaned by carefully washing in "piranha solution." A permanent magnet of field strength H= 1.5T was placed just below the working electrode before the measurements were conducted. The field strength on the Ni surface was measured by a digital Gauss meter and was found to be 0.35T on the surface of Ni.

ACKNOWLEDGMENTS. D.M., T.Z.M., and R.N. acknowledge the partial support of the German Israel Science Foundation, the MINERVA Foundation, the Schmidt Minerva Center, and the Israel Science Foundation.

1. Hore PJ (2012) Are biochemical reactions affected by weak magnetic fields? *Proc Natl Acad Sci USA* 109(5):1357–1358.
2. Maeda K, et al. (2012) Magnetically sensitive light-induced reactions in cryptochrome are consistent with its proposed role as a magnetoreceptor. *Proc Natl Acad Sci USA* 109(13):4774–4779.
3. Naaman R, Waldeck DH (2012) Chiral-induced spin selectivity effect. *J Phys Chem Lett* 3(16):2178–2187.
4. Göhler B, et al. (2011) Spin selectivity in electron transmission through self-assembled monolayers of double-stranded DNA. *Science* 331(6019):894–897.
5. Xie ZT, et al. (2011) Spin specific electron conduction through DNA oligomers. *Nano Lett* 11(11):4652–4655.
6. Ray SG, Daube SS, Leitus G, Vager Z, Naaman R (2006) Chirality-induced spin-selective properties of self-assembled monolayers of DNA on gold. *Phys Rev Lett* 96(3):036101.
7. Guo AM, Sun QF (2012) Spin-selective transport of electrons in DNA double helix. *Phys Rev Lett* 108(21):218102.
8. Gutierrez R, Diaz E, Naaman R, Cuniberti G (2012) Spin-selective transport through helical molecular systems. *Phys Rev B* 85:081404.
9. Jin Y, Friedman N, Sheves M, He T, Cahen D (2006) Bacteriorhodopsin (bR) as an electronic conduction medium: Current transport through bR-containing monolayers. *Proc Natl Acad Sci USA* 103(23):8601–8606.
10. Sepunaru L, Friedman N, Pecht I, Sheves M, Cahen D (2012) Temperature-dependent solid-state electron transport through bacteriorhodopsin: Experimental evidence for multiple transport paths through proteins. *J Am Chem Soc* 134(9):4169–4176.
11. Berthoumieu O, et al. (2012) Molecular scale conductance photoswitching in engineered bacteriorhodopsin. *Nano Lett* 12(2):899–903.
12. Mukhopadhyay P, Zuber G, Wipf P, Beratan DN (2007) Contribution of a solute's chiral solvent imprint to optical rotation. *Angew Chem Int Ed Engl* 46(34): 6450–6452.
13. Barbosa MR, Real SG, Vilche JR, Arvia AJ (1988) Comparative potentiodynamic study of nickel in still and stirred sulfuric acid-potassium sulfate solutions in the 0.4–5.7 *p*H range. *J Electrochem Soc* 135(5):1077–1085.
14. Mekhalif Z, Riga J, Pireaux JJ, Delhalle J (1997) Self-assembled monolayers of n-isodecanthiol on electrochemical modified polycrystalline nickel surface. *Langmuir* 13(8): 2285–2290.
15. Mekhalif Z, Laffineur F, Couturier N, Delhalle J (2003) Elaboration of self-assembled monolayers of n-alkanethiols on nickel polycrystalline substrates: Time, concentration, and solvent effects. *Langmuir* 19(3):637–645.
16. Zhang L, Lin X (2005) Electrochemical behavior of a covalently modified glassy carbon electrode with aspartic acid and its use for voltammetric differentiation of dopamine and ascorbic acid. *Anal Bioanal Chem* 382(7):1669–1677.
17. Vanossi D, et al. (2012) Functionalization of glassy carbon surface by means of aliphatic and aromatic amino acids. An experimental and theoretical integrated approach. *Electrochim Acta* 75:49–55.
18. Brooksby PA, Anderson KH, Downard AJ, Abell AD (2010) Electrochemistry of ferrocenoyl β-peptide monolayers on gold. *Langmuir* 26(2):1334–1339.
19. Chen W (2005) Electroconformational denaturation of membrane proteins. *Ann N Y Acad Sci* 1066:92–105.
20. Freedman KJ, Haq SR, Edel JB, Jemth P, Kim MJ (2013) Single molecule unfolding and stretching of protein domains inside a solid-state nanopore by electric field. *Scientific Rep* 3:1638.
21. Qi X-L, Zhang S-C (2010) The quantum spin Hall effect and topological insulators. *Phys Today* 63(1):33–38.
22. Oesterhelt D, Stoeckenius W (1974) Isolation of the cell membrane of Halobacterium halobium and its fractionation into red and purple membrane. *Methods Enzymol* 31:667–678.
23. Oesterhelt D, Schuhmann L, Gruber H (1974) Light-dependent reaction of bacteriorhodopsin with hydroxylamine in cell suspensions of Halobacterium halobium: Demonstration of an apo-membrane. *FEBS Lett* 44(3):257–261.